

# Collisionless Damping of Fast MHD Waves in Magetorotational Winds

T. K. Suzuki<sup>1</sup>, H. Yan<sup>2</sup>, A. Lazarian<sup>2</sup>, & J. P. Cassinelli<sup>2</sup>

## ABSTRACT

We propose collisionless damping of fast MHD waves as a important mechanism for the heating and acceleration of winds from rotating stars. Stellar rotation causes magnetic field lines anchored at the surface to form a spiral pattern and magnetorotational winds can be driven. If the structure is a magnetically dominated, fast MHD waves generated at the surface can propagate almost radially outward and cross the field lines. The propagating waves undergo collisionless damping owing to interactions with particles trapped in magnetic mirrors that are formed by the waves themselves. The energy damping rate is especially effective where the angle between the wave propagation and the field lines becomes moderately large ( $\sim 20$  to  $80^\circ$ ). The angle tends naturally to increase into this range because the field in magnetorotational winds develops an increasingly large azimuthal component. The dissipation of the wave energy produces heating and acceleration of the outflow. We show using specified wind structures that this damping process can be important in both solar-type stars and massive stars that have moderately large rotation rates, provided that there are high temperatures in the outer atmosphere, which we treat as extended hot coronae.

*Subject headings:* magnetic fields – plasma – magnetohydrodynamics – stars : winds – waves

## 1. Introduction

A wide range of stellar classes are thought to have hot plasmas with temperatures greater than  $10^6$  K in their atmosphere. Main sequence stars with low to intermediate mass, including the sun, are known to possess hot coronae, and stellar winds emanate from there by thermal expansion most likely enhanced by magnetic wave energy deposition. Magnetic fields generated by dynamo mechanisms in these stars are likely brought to the surface by magnetic buoyancy in the convection zones (Parker 1966), and the fields play a major role in the structure of the outer atmosphere. In a static atmosphere, the gas pressure,  $p$ , falls exponentially with a scale height  $H$ , but the magnetic field,  $B$ , generally decreases more slowly, as a power-law with radius  $r$  to satisfy conservation of magnetic flux. As a result, the magnetic pressure,  $B^2/8\pi$ , can eventually dominate thermal pressure from a certain radius outward, even though the thermal pressure dom-

inates in regions nearer the photosphere. Thus in the outer regions the dissipation of the magnetic energy can greatly influence the energetics and dynamics of the atmosphere and wind, producing in some way, the heating of coronae and the wave acceleration of stellar winds. We intend to explore a wave damping process that can produce the heating and acceleration.

It is now becoming more evident that the heating and driving effects of magnetic fields is not confined only to cool stars, but can be important in the more massive early type stars as well. For many years it had been believed that dynamo generated magnetic fields would not exist on hot stars, and that the winds from these objects were produced only as a result of radiation pressure gradients. Unlike the cooler stars, the hot massive stars do not have an outer convection zone, so the mechanism for the rise of magnetic fields and the source of mechanical energy for coronal heating are not present. However, early UV spectra of the stars showed lines from anomalously high ionization stages (Lamers & Morton 1976). This superionization could be explained as resulting from X-ray ionization by the Auger Effect (Cassinelli & Olson 1979). It was soon realized from satellite observations that essentially all

<sup>1</sup>Department of Physics, Kyoto University, Kitashirakawa, Kyoto, 606-8502, Japan; JSPS Research Fellow; stakeru@scphys.kyoto-u.ac.jp

<sup>2</sup>Department of Astronomy, University of Wisconsin, 475 N. Charter St., Madison, WI 53706; yan@astro.wisc.edu

O and B stars are X-ray sources (Seward et al. 1979), but the nature of the source of the X-rays remained a mystery. (Cassinelli & Swank 1979) provided arguments that perhaps there are both shocks in the winds (as proposed by Lucy 1982), as well as hot coronal regions at the base of the winds. This idea that there are two contributors to the X-ray emission has persisted (Waldron and Cassinelli, 2000). Also, in the case of B near main sequence stars, Cohen et al (1996), found that the X-ray emission measure was comparable or larger than that of a theoretically predicted wind, and hence the coronal component of the X-ray emission could be dominant for these stars. As for the magnetic fields in the outer atmospheres and winds, some direct measurements have been made in near main sequence B stars with fields of about 300 Gauss (Donati et al. 2001). Charbonneau and MacGregor (2001) have shown that fields can be generated by a dynamo operating at the interface between the convective core and the radiative envelope in early type stars. MacGregor and Cassinelli (2003) have shown that such fields can buoyantly rise through the radiative zone to the surface of hot stars. In addition there is a wide variety of observational evidence that hot stars have magnetic fields (Henrichs 2002). Thus, there appears to be a greater similarity between hot and cool stars than had been envisioned, and it is both timely and useful to consider the processes by which magnetic fields can heat and accelerate winds across the HR diagram. Here the focus is on structures in which the field is configured in the form of a spiral, as naturally arises from the rotation of a star with a magnetic field embedded at the surface.

Magnetohydrodynamic (MHD) waves are widely regarded as producing mechanisms that play a role in the heating and acceleration of the outer atmospheric plasmas. Surface turbulence and transient activities (e.g. Sturrock 1999) excite MHD waves at the surface of the sun. It is natural to expect that similar excitation phenomena occur on other stars that have surface magnetic fields. Outwardly propagating MHD waves carry Poynting flux energy, and any dissipation of this flux directly leads to conversion from magnetic energy to thermal and kinetic energy in upper atmosphere. There are numerous studies of wave heating in the solar corona / wind (e.g. Belcher 1971) and in stellar coronae / winds (e.g. Hartmann & MacGregor 1980). MHD waves are discussed in regards to pulsar winds as well (Lyubarsky 2003).

Stellar surface motions are likely to be the source

of the MHD wave energy. Turbulence in a localized source region creates a flow of wave-like motions that can be decomposed into three types of MHD waves: fast, Alfvén, and slow modes (see Cho & Lazarian 2003). In a magnetically dominated plasma, the slow mode essentially corresponds to acoustic wave, hence, it probably does not contribute the dominant amount of heating to the plasma. The fast and Alfvén modes, however, can play a dominant role since their wave energies can easily exceed the thermal energy. These two modes show quite different natures. The Alfvén waves propagate as transverse waves only along the field lines, while fast waves can propagate almost isotropically. The properties of fast mode wave can change with distance because they depend on the direction of the wave relative to the magnetic field line. The component which is traveling along the field line is transverse, as is the case for the Alfvén mode, but the fast wave mode becomes increasingly compressive as the angle,  $\theta$ , between the wave propagation vector and the field line increases.

Some of the properties of the wave propagation are affected by the rotation of the star because the rotation causes the magnetic field lines that are rooted on the star to form a spiral pattern (fig. 1) (Weber & Davis 1967; Belcher & MacGregor 1976). In the solar wind, the field is usually pictured as developing a so-called Parker spiral (Parker 1963). This spiral arises in spite of the relatively slow rotation of the Sun. More tightly wrapped spiral patterns should form in the winds of stars that rotate faster, such as younger solar-like stars and massive stars. Thus, it is important and interesting to study outward propagation of the fast MHD waves in magnetorotational winds of rapidly rotating stars.

Let us consider outgoing fast waves that have been generated by some surface activity. The fast waves will travel in almost radially without being refracted provided that the magnetic energy in the plasma dominates the thermal energy. However, as the wave travels away from the surface, the angle of propagation,  $\theta$ , increases monotonically and the wave character changes accordingly. The way in which the dissipation of the waves is influenced by this variation of  $\theta$  is described in (§2), and there we discuss how the stellar rotation plays a dominant role in controlling the wave dissipation and subsequent heating of the stellar atmosphere.

An important aspect in the discussion of stellar plasmas is that they are generally collisionless except in regions very near the surface. This is the case because the mean free path with respect to Coulomb col-

lision;

$$l_{\text{mfp}} = 9.38 \times 10^7 \text{ cm} \frac{(T/10^6 \text{ K})^2}{(n/10^8 \text{ cm}^{-3})}, \quad (1)$$

is larger than wave length, and thus it is essential for us to consider collisionless processes in the wave dissipation. In fact, it has recently been shown (Yan & Lazarian 2004), that the fast wave mode suffers collisionless damping. Furthermore, the damping rate sensitively depends on  $\theta$  (§2). To date, however, this damping process has not been applied to magnetically dominated winds. It is the goal of this paper to investigate the importance of collisionless damping for both the heating and acceleration of stellar coronae in which the field has the configuration of a magnetorotational wind.

## 2. Damping of Fast MHD Waves

In this section, we summarize the physical process of collisionless damping of the fast MHD waves, and we introduce the damping rate. It is useful to compare the damping by this process with one that has often been considered in the literature (Hollweg 1982; Suzuki 2004); the damping of waves by the formation of a fast shock train by steepening of the wave fronts. We discuss circumstances in coronae under which the collisionless damping becomes more important than the shock steepening process.

As discussed in Ginzburg (1961), the nature of collisionless damping can be considered analogous to the creation of radiation by charged particles in magnetic field. The charged particles can emit electromagnetic waves both by their acceleration (which produces cyclotron radiation) and by the Cherenkov effect. By the inverse of these two processes charged particles can absorb the radiation. More generally plasmas can absorb energy of plasma waves by gyroresonance process or by a process analogous to the Cherenkov effect. It is the latter that is of interest to us here, as it leads to a dissipation of the plasma waves propagating through a corona by a wave-particle interaction and thereby to a heating and acceleration of the particles that compose the plasma.

The resonance of the wave with the gyroresonance frequency of ambient thermal ions causes a damping of those wave modes that have a frequency close to the ion-cyclotron frequency (e.g. Leamon et al. 1998). The thermal particles can also be accelerated by an oscillating parallel electric field, as is the case for Landau damping of a wave. In this process fast parti-

cles, which can be pictured as surfing on a plasma wave, absorb the wave energy. Similar mechanism also operates for moving magnetic mirrors instead of the electric field. Yan and Lazarian (2004) discuss collisionless damping of fast MHD waves by an interaction between the thermal particles and a magnetic mirror, often called transit time damping (TTD). It is this novel TTD effect that we will be applying to magnetorotational winds. In this paper, we are considering the TTD of fast MHD waves in a magnetically dominated medium. Such a medium is commonly called a low  $\beta$  plasma, where  $\beta$  is as usual the ratio of the gas pressure  $p_g = \rho a^2$ , to the magnetic pressure,  $p_b = B^2/8\pi$ ,

$$\beta \equiv \frac{p_g}{p_b} = \frac{8\pi\rho a^2}{B^2}, \quad (2)$$

where  $B$  is the magnetic field strength,  $\rho$  is the ambient gas density, and  $a$  is the isothermal sound speed.

Figure 2 illustrates magnetic mirrors formed by traveling fast MHD waves with different  $\theta$ . Particles with parallel velocity,  $v_{\parallel}$ , in the range

$$v_{\parallel,c} - \Delta v_{\parallel,c} \leq v_{\parallel} \leq v_{\parallel,c} + \Delta v_{\parallel,c}, \quad (3)$$

are trapped by magnetic mirrors. Here,  $v_{\parallel,c}$  is the particle parallel speed which meets the Cherenkov condition,  $v_{\parallel,c} = \omega/k_{\parallel}$ , where  $\omega$  and  $k_{\parallel}$  are wave frequency and wave number parallel to magnetic field line, respectively, which are determined by the fast mode speed. Width in velocity space,  $\Delta v_{\parallel,c}$ , of the trapped particles is related to fluctuation component of field strength,  $\Delta B$ , accompanying with the mirrors as  $\Delta v_{\parallel,c} \propto \Delta B^{1/2}$  (e.g. Boyd & Sanderson 2003). (note that variation of a distance between two field lines in fig.2 gives  $\Delta B$ )

A few points should be noted in regards to the interactions between the particles and the moving mirrors. First, the above condition for trapping by magnetic mirrors favors plasmas which have a  $\beta$  value not too far below unity. This is because the parallel speeds of the surfing particles needs to be comparable to fast mode speed for the resonance to occur. For example, if the plasma  $\beta$  is too low, which is equivalent to too low sound speed, only a insignificant fraction of the particle speed distribution function will have the large values required by condition eq. (3). Second, large fluctuation of the magnetic field is favored for the efficient trapping of the particles. Case (2) in fig.2 illustrates a more extreme bottle shape with larger  $\Delta B$

than case (1) and we see that it gives rise to a larger  $\Delta v_{\parallel,c}$ . As a result more particles would be trapped for Case (2).

Among the trapped particles, the most particles have  $v_{\parallel} < v_{\parallel,c}$  initially since  $v_{\parallel,c}$  is larger than the average particle velocity, *i.e.* sound speed. On the other hand, their average speed eventually becomes  $v_{\parallel,c}$  after reflection at both edges of the magnetic bottles. This indicates that the particles gain energy, or equivalently, a dissipation of the wave would occur by collisionless mechanism. As is shown in Yan and Lazarian (2004) (following Ginzburg, 1961), the damping rate  $\gamma_d$  of fast wave modes with frequency  $\omega$  for a given  $\beta \ll 1$  and  $\theta \sim 1$  for the Maxwell-Boltzmann particle distribution is

$$\gamma_d = \frac{\sqrt{\pi\beta}}{4} \omega \frac{\sin^2 \theta}{\cos \theta} \times \left[ \sqrt{\frac{m_e}{m_H}} \exp\left(-\frac{m_e}{m_H \beta \cos^2 \theta}\right) + 5 \exp\left(-\frac{1}{\beta \cos^2 \theta}\right) \right], \quad (4)$$

where  $m_H$  and  $m_e$  are the hydrogen and electron masses.

The Upper panel of fig. 3 presents  $\gamma_d$  divided by  $\omega$  as a function of the angle  $\theta$  for different values of  $\beta$ , from  $\beta = 0.1$  and  $0.01$ . These are shown in comparison with the damping rate associated with a shock train that is usually used for such discussions. (see the Appendix for a discussion of the the damping of waves by the shocks). The rate of the collisionless damping is independent of wave amplitude,  $\delta B$ , because it is a linear process, while it depends on the plasma  $\beta$  as was described above. The collisionless damping shows a quite sensitive behavior on  $\theta$ ; the damping rate increases more rapidly than the steepening in the range  $\theta$  up to  $\theta \lesssim 80^\circ$ , but then the collisionless damping suddenly decreases as  $\theta$  comes closer to  $90^\circ$ . This behavior can be interpreted by considering two competing factors. In general the damping increases with  $\theta$  because a magnetic mirror tends to be formed in a more efficient way, as is illustrated in fig. 2. Thus, more particles can be trapped and interact with the wave to cause the dissipation. However, when  $\theta$  approaches to  $90^\circ$ ,  $k_{\parallel}$  becomes small the resonance condition requires a large  $v_{\parallel}$ . Hence, most thermal particles will no longer be in resonance with the wave, so the damping rate decreases sharply in the  $\theta$  near  $90^\circ$  regime.

On the other hand, the damping caused by the shocks is dependent on  $\delta B$  because it is a nonlinear process, but it is almost independent of the plasma  $\beta$

value. Although the damping rate by the shock steepening also increases with  $\theta$  as in the collisionless process, the increase is more gradual. The gradual increase of the damping rate is due to change of wave character. A fast wave traveling along a field line, *i.e.*  $\theta = 0^\circ$ , is transverse mode, but as  $\theta$  increases, the wave contains a longitudinal, *i.e.* compressional, component, implying that it becomes more dissipative. As a result, fast shocks that have a larger  $\theta$  also have a larger compression, so that the damping by shocks is more efficient for larger  $\theta$  as well. Nonetheless, the variation is still less dependent on  $\theta$  than for the case of collisionless damping.

Figure 3 shows conditions under which collisionless damping is as important as or more important than the shock steepening process. The comparison is further illustrated in the lower panel of fig. 3 which shows on a  $\theta$  versus  $\beta$  plane where the collisionless process exceeds the shock steepening process, for two cases,  $\delta B/B = 0.1$  (cross hatched) and  $\delta B/B = 0.01$  (single hatched).

Note that the collisionless process tends to becomes more important for larger values of  $\theta$ , except when  $\theta$  is nearly  $90^\circ$  and except also for cases in which the  $\beta$  value is small. As is shown, a fast wave with amplitude  $\delta B/B = 0.01$  will dissipate predominantly by collisionless damping over a wide range of  $\theta$ . Even for the case in which  $\delta B/B = 0.1$ , the collisionless damping is seen to be more important for  $\beta \simeq 0.1$  in an angular region of  $60^\circ \lesssim \theta < 90^\circ$ . These results show that there are interesting physical conditions under which collisionless damping should from now on be taken to be the primary process for wave dissipation.

The results in the plots have shown that the collisionless damping can be comparable or more important than shock steepening for the damping of fast waves. Collisionless damping could dominate even more-so, because the damping by the shock steepening could be smaller than we have assumed, for the following reasons. First, when a sinusoidal wave is excited initially, it takes some time for it to steepen to form the shocks before the shock dissipation process can begin. Whereas the collisionless damping works immediately, even for the case of sinusoidal waves. Second, the collisionless effects can themselves modify the shock dissipation. In general astrophysical circumstances, each shock in a shock train is considered collisionless, so the plasma is not thermalized by Coulomb collisions, but rather the plasma is randomized because of fluctuations in the magnetic field. However

shock dissipation is estimated using MHD treatments. The collisionless effects are often supposed to make the damping less efficient than would be derived from MHD assumptions. We conclude from this section that our results indicate that it is important to account for collisionless damping of the fast modes for realistic and interesting astrophysical situations.

### 3. Model for Magnetorotational Winds

Let us consider the outward propagation of the fast MHD waves for the case of magnetorotational stellar winds. Figure 1 depicts propagation of the fast MHD waves in the rotational winds seen from the pole. Here we adopt a simple split monopole configuration for the magnetic fields and assume that the magnetic axis coincides with the stellar spin axis. Spiral magnetic fields are formed in the equatorial region by the stellar rotation (Weber & Davis 1967; Belcher & MacGregor 1976). We can also reasonably assume that the ideal MHD condition holds in the stellar atmosphere. These are common assumptions for the equatorial region of a magnetorotational wind.

The plasma itself cannot move across the field lines. However, the fast MHD waves can propagate almost isotropically in a low  $\beta$  plasma. In particular, they can propagate radially, crossing the field lines as illustrated in the figure. Also shown is the increase in the angle  $\theta$  as the wave travels away from the surface. Where the angle  $\theta$  is large, the fast waves suffer collisionless damping, as we discussed in the previous section, as long as the wave length,  $\lambda$ , is short enough to satisfy collisionless condition,

$$\lambda < l_{\text{mfp}}. \quad (5)$$

where  $l_{\text{mfp}} = 9.38 \times 10^7 \text{ cm} \frac{(T/10^6 \text{ K})^2}{(n/10^8 \text{ cm}^{-3})}$ . For example, if we consider a fast mode wave with period 1s, with a phase speed is 1000 km/s traveling in plasma with a temperature of  $2 \times 10^6$  K, the collisionless condition that must be satisfied for the particle density is  $n \lesssim 10^8 \text{ cm}^{-3}$ . In the case of the sun, this density condition holds even in the inner corona. As a result, the wave dissipation process directly leads to heating and acceleration of wind plasma and may have an effect on the wind structure.

In this section, we present a model to explore the collisionless damping of the fast mode for the case of magnetorotational winds. As we are just beginning to develop an understanding of the basic collisionless

damping process, it is too soon to be aiming for a complete and self consistent picture. For example, there are other processes such as shock dissipation argued in the previous section that may still be important. We choose to estimate the energy and momentum that is transferred by the fast wave dissipation in the case of a fixed background wind. Then we can discuss the likely influence on the wind energetics and dynamics.

#### 3.1. Approximated Wind Structure

Here we describe a practical method for constructing approximate wind structures in the equatorial plane of the magnetorotational winds. We assume that the wind is isothermal at a temperature  $T$ , and we assume that all the physical quantities depend spatially only on the radial distance,  $r$  in the equatorial plane. For the split monopole magnetic field, the conservation of magnetic flux,  $\nabla \cdot \mathbf{B} = 0$ , fixes radial component of the magnetic field,

$$B_r = \left( \frac{R_\star}{r} \right)^2 B_{r,0}, \quad (6)$$

where  $R_\star$  is stellar radius and  $B_{r,0}$  is radial field strength at the surface where  $r = R_\star$ . It is empirically known that radial velocity distribution of stellar winds can be represented by the “beta velocity law” (here we use the power  $\eta$  to avoid confusion with the plasma  $\beta$  ratio that we have used throughout), thus

$$v_r = v_\infty \left( 1 - \frac{R_\star}{r} \right)^\eta, \quad (7)$$

where  $\eta \simeq 0.5\text{--}3$  (Lamers & Cassinelli 1999). If the rotation is slow, terminal velocity,  $v_\infty$ , is of order the escape velocity,  $v_{\text{esc},0} \simeq \sqrt{\frac{2GM_\star}{R_\star}}$ , where  $M_\star$  is stellar mass.

In rapid rotating stars,  $v_{\text{esc},0}$  may not a good indicator of the terminal velocity, as  $v_\infty > v_{\text{esc},0}$  because the wind is significantly affected by acceleration from the magnetorotational forces, (e.g. Lamers & Cassinelli 1999). For these cases,  $v_\infty$  is better estimated by the Michel velocity (Michel 1967), which is defined as

$$v_M = \left( \frac{r^4 B_r^2 \Omega^2}{\dot{M}_E} \right)^{1/3} = \left( \frac{R_\star^4 B_{r,0}^2 \Omega^2}{\dot{M}_E} \right)^{1/3}, \quad (8)$$

where  $\Omega$  is angular speed of stellar rotation and  $\dot{M}_E$  is equatorial mass flux rate multiplied by  $4\pi r^2$  and we use,

$$\dot{M}_E = 4\pi \rho v_r r^2 (= \text{const.}) \quad (9)$$

In this paper we adopt

$$v_\infty = \max(v_{\text{esc},0}, v_M). \quad (10)$$

It should be noted that  $v_\infty$  can be estimated by the surface values since both  $v_{\text{esc},0}$  and  $v_M$  are determined at  $r = R_\star$ . We, from now, conventionally call cases with  $v_{\text{esc},0} > v_M$ ,  $v_{\text{esc},0} \simeq v_M$ , and  $v_{\text{esc},0} < v_M$  slow, moderate, and fast magneto-rotators, respectively.

We can determine azimuthal field component,  $B_\phi$ , for given  $\Omega$  by the induction equation as (see Lamers & Cassinelli 1999)

$$\frac{B_\phi}{B_r} = \frac{v_\phi - r\Omega}{v_r}. \quad (11)$$

Azimuthal velocity,  $v_\phi$ , is derived from conservation of angular momentum as

$$v_\phi = r\Omega \frac{\frac{v_r^2 \mathcal{L}}{r^2 \Omega} - v_{A,r}^2}{v_r^2 - v_{A,r}^2} = r\Omega \frac{\frac{r_A^2}{r^2} v_r^2 - v_{A,r}^2}{v_r^2 - v_{A,r}^2}, \quad (12)$$

where  $\mathcal{L}$  is specific angular momentum,  $v_{A,r} = \frac{B_r}{\sqrt{4\pi\rho}}$  is radial Alfvén speed, and  $r_A$  is Alfvén point at which  $v_r = v_{A,r}$ . Thus, we have set the structures of the magnetorotational winds for given  $M_\star$ ,  $R_\star$ ,  $\dot{M}_E$ ,  $B_{r,0}$  and  $S_0$ , where  $S_0$  is spin normalized by Kepler velocity,  $\Omega_K = \sqrt{\frac{GM_\star}{R_\star}}$ :

$$S_0 \equiv \frac{\Omega}{\Omega_K} \quad (13)$$

### 3.2. Wave Propagation

We introduce formulation describing propagation of the fast MHD waves with dissipation in the magnetorotational winds under the WKB approximation. We only consider magnetically dominated *i.e.*, low  $\beta$  plasmas. Accurately speaking, refraction affects the wave propagation; the fast wave propagates toward a region with smaller phase speed,  $v_f$ , defined as<sup>3</sup>

$$v_f = \frac{B}{\sqrt{8\pi\rho}} \left[ 1 + \frac{4\pi\rho a^2}{B^2} + \sqrt{\left(1 + \frac{4\pi\rho a^2}{B^2}\right)^2 - \frac{4B_r^2}{B^2} \frac{4\pi\rho a^2}{B^2}} \right]^{1/2}, \quad (14)$$

which corresponds to a direction away from the field line. However, in the case of a low  $\beta$  plasma we

<sup>3</sup>Although adiabatic sound speed should appear here, we use isothermal sound speed,  $a$ , as we assume the isothermal atmosphere.

can reasonably assume that the fast waves propagate radially without suffering the refraction, because  $v_f \simeq \frac{B}{\sqrt{4\pi\rho}}$  is almost independent of  $\theta$ , where  $B = \sqrt{B_r^2 + B_\phi^2}$ .

The energy flux of MHD waves in fluids moving with velocity,  $\mathbf{v}$  is written as (Jacques 1977)

$$\mathbf{F}_w = \mathbf{V}_g \mathcal{E}_w + \mathbf{v} \cdot \mathbf{p}_w \quad (15)$$

where  $\mathcal{E}_w$  is wave energy density,  $\mathbf{V}_g$  is group velocity, and  $\mathbf{p}_w$  is wave pressure. Wave amplitude,  $\delta v$ , gives,  $\mathcal{E}_w = \frac{1}{2} \rho \delta v^2$ .  $\mathbf{F}_w$  changes according to work done by  $\mathbf{p}_w$  and damping loss,  $-Q_w$ , in the steady state condition,

$$\nabla \cdot \mathbf{F}_w - \mathbf{v} \cdot (\nabla p_w) = -Q_w. \quad (16)$$

Note that  $Q_w$  works as a heating term for the surrounding plasma. We focus on fast MHD waves in the low  $\beta$  plasma. Radial components of the pressure gradient,  $\nabla p_{fw}$ , and the energy flux,  $\mathbf{F}_{fw}$ , can be expressed as (Jacques 1977)

$$(\nabla \cdot \mathbf{p}_{fw})_r = \left( \frac{1}{2} + \sin^2 \theta \right) \frac{d\mathcal{E}_{fw}}{dr} + \frac{3\mathcal{E}_{fw}}{r} \sin^2 \theta \quad (17)$$

and

$$F_{fw,r} = \mathcal{E}_{fw} \left[ \left( \frac{3}{2} + \sin^2 \theta \right) v_r + v_f \right]. \quad (18)$$

The term  $\gamma_d$  in eq. (4) is defined as the damping rate with respect to normalized amplitude,  $\delta w \equiv \delta v/v_f$ . Then, substitutions of eqs.(17) and (18) into eq. (16) give the variation of  $\delta w$  in the stellar winds, of

$$\begin{aligned} \frac{d}{dr}(\delta w) = -\delta w & \left[ \frac{\gamma_d}{v_r + v_f} + \frac{1}{2\rho} \frac{d\rho}{dr} + \frac{1}{v_f} \frac{dv_f}{dr} \right. \\ & + \frac{1}{2(v_r + v_f)} \left\{ \frac{(3 - \sin^2 \theta)v_r + 2v_f}{r} \right. \\ & \left. \left. + \frac{d}{dr} \left\{ \left( \frac{3}{2} + \sin^2 \theta \right) v_r + v_f \right\} \right\} \right], \end{aligned} \quad (19)$$

The first term on the right hand side denotes the collisionless damping. The second term indicates the amplification that occurs in a stratified atmosphere in which the density  $\rho$  is decreasing. The third term appears because  $v_f$  is used for the normalization of  $\delta w$ . The fourth term is due to geometrical expansion of flow tubes and the variation of  $v_f$ .

For a given wave frequency,  $\omega$ , then  $\gamma_d = \gamma_d(\beta, \theta, \omega)$  can be determined by the plasma  $\beta$  (eq. 2) and the angle  $\theta$ . For the assumed radial propagation, the spiral

angle between the propagation direction and the field line can be expressed as

$$\theta = \tan^{-1} \left( \frac{B_\phi}{B_r} \right). \quad (20)$$

Thus we see that the damping rate,  $\gamma_d$ , is fully determined by the background wind properties.

At the surface of the star, we have the initial conditions of outgoing fast waves with an amplitude,  $\delta w_0 \equiv \delta v_0/v_{f,0}$ , and a period,  $\tau (= 2\pi/\omega)$ . In the following calculations, we consider the results using  $\delta w_0 = 0.1$  as a fiducial value. In a region close to the surface, the plasma is generally collisional, i.e.  $\lambda (= v_f \tau) < l_{\text{mfp}}$ . In this region, eq. (19), with the collisionless damping, is not applicable, so we assume  $\gamma_d = 0$  when solving eq. (19). Even without the damping,  $\delta w$  decreases because of the rapid increase of  $v_f$ , (see §4). As a result, other damping processes should not be effective either, so our treatment has acceptably isolated the collisionless damping case. Once the collisionless condition, eq. (5), is satisfied at  $r = r_{\text{cl}}$  and beyond, we can start the outward integration of eq. (19) to determine  $\delta w$ . Using this, we can estimate heating,  $Q_w$ , and find the acceleration,  $-\frac{dp_w}{dr}$ , that is caused by the dissipation of the fast MHD waves.

## 4. Results

There are two important requirements for our model of the collisionless dissipation of the fast MHD waves in the magnetorotational winds. First, a sufficiently large rotation rate is required to create the moderate  $\theta$  that is needed for the wave dissipation. Second, stellar winds with moderately low plasma  $\beta$  values, (i.e.  $\beta \sim 0.01 - 0.1$ ) are favorable, because the fast waves, which are essentially magnetic waves, can be dominant only for low  $\beta$  plasmas, although the dissipation is suppressed if the  $\beta$  value is too small. (eq. (4)).

### 4.1. Solar-type Stars

Moderately low  $\beta$  winds are found in the coronal winds of low to intermediate mass stars. Although the Sun is certainly one of the candidates in the sense that it is a moderate to late type star, it has a rotation rate that is too slow to produce the large  $\theta$  assumed in our discussion. It is known from observations of spectral lines that early type stars are commonly fast rotators. This is because such a star tends to be rotating quickly after its initial collapse and formation, the lives are

rather short, and thus that the massive stars are able to persist in having rapid rotation. Observations of F-K stars in open clusters (Barnes 2003) show that stars with age  $\lesssim 100$  Myr have as large spin <sup>4</sup> as  $S_0 \simeq 0.5$ . Thus these are good classes of stars for us to be considering here.

Figure 4 presents result of moderate magnetorotational wind for  $S_0 = 0.15$  in a solar-mass star ( $M = 1M_\odot$  and  $R = 1R_\odot$ ). We adopt  $B_{r,0} = 8$  G and  $T = 2 \times 10^6$  K as typical values. A larger mass loss rate,  $\dot{M}_E = 2 \times 10^{-13} M_\odot \text{yr}^{-1}$ , is employed than the present solar value,  $\dot{M} \simeq 2 \times 10^{-14} M_\odot \text{yr}^{-1}$ , because young solar-like stars are found to have larger mass loss rate (Wood et al. 2002) possibly as a result of their enhanced coronal activities or stellar rotation.

On the left we show the wind structures as a function of  $r$ . The top panel shows velocity structure,  $v_r$  and  $v_\phi$ , compared with  $v_f$  and rigid rotation speed  $r\Omega$ .  $v_M = 1018$  km/s, which is larger than the escape speed,  $v_{\text{esc},0} = 617$  km/s, is selected as  $v_\infty$  in this case, following eq. (10). We adopt  $\eta = 3$  for the velocity law index (eq:7), although we find that  $\eta$  affects the results only weakly. The difference between  $v_\phi$  and the solid body rotation,  $r\Omega$ , leads to the spiral pattern. The middle panel shows that the angle  $\theta$  increases monotonically up to  $\gtrsim 70^\circ$ . The bottom panel presents the plasma  $\beta$  value (eq. (2)), and it shows that moderately low- $\beta$  circumstances are in fact realized for these calculations.

Once we have fixed the wind structure, we can solve propagation of the fast waves by using eq. (19). Results for wave periods  $\tau = 1, 10, 100$  s are shown on the right of fig.4. The top panel exhibits variation of  $\delta w$  (solid) in comparison with the no-dissipation case (dashed). While  $\delta w$  initially decreases due to a rapid increase of  $v_f$  to satisfy the wave energy equation (16), it is eventually amplified through outward propagation in decreasing density. Waves with shorter  $\tau$  suffer greater damping per unit length, so that they dissipate faster.

The middle panel shows a role of the wave dissipation in wind energetics. An equation describing variation of internal energy per unit mass,  $e$ , is written as

$$v_r \frac{de}{dr} + \frac{a^2}{r^2} \frac{d}{dr} (r^2 v_r) - Q_w = 0, \quad (21)$$

where second term denotes adiabatic loss and a third term is heating by the wave dissipation. We plot the

<sup>4</sup>  $S_0 = 0.005$  for the sun.

heating term for different  $\tau$  (solid) compared with the adiabatic cooling term (dashed), although we do not explicitly solve the equation. The figure illustrates that regions that are heated by the waves depend on the value of  $\tau$ . The waves with the smaller values of  $\tau$  heat the inner regions. The heating exceeds the adiabatic cooling in the respective regions, and this indicates that the assumed temperature ( $= 2 \times 10^6$  K) could indeed be maintained sufficiently by the wave dissipation. In the real situation, the heating could be distributed more uniformly than shown in fig. 4 if we were to take into account the wave spectrum and thermal conduction as well, which will be discussed later (§5.1).

The bottom panel shows the wind dynamics. The equation of momentum density is

$$\frac{d}{dr} \left( \frac{v_r^2 + v_\phi^2}{2} \right) + \frac{1}{\rho} \frac{dp_g}{dr} + \frac{1}{\rho} \frac{dp_{fw}}{dr} + \frac{GM_\star}{r^2} - \frac{d}{dr} \left( \frac{r\Omega B_r B_\phi}{4\pi\rho v_r} \right) = 0, \quad (22)$$

(Lamers & Cassinelli 1999), and the second and third terms are acceleration by the gas and the wave pressure, respectively. A fifth term accounts for magnetorotational acceleration and it consists of centrifugal force and acceleration owing to the slinging effect of the rotating magnetic field. We compare these three terms in ratios relative to the gravitational acceleration, i.e.

$$\begin{aligned} \Gamma_g &= \left| \frac{1}{\rho} \frac{dp_g}{dr} / \frac{GM_\star}{r^2} \right|, \\ \Gamma_w &= \left| \frac{1}{\rho} \frac{dp_{fw}}{dr} / \frac{GM_\star}{r^2} \right|, \\ \Gamma_b &= \left| \frac{d}{dr} \left( \frac{r\Omega B_r B_\phi}{4\pi\rho v_r} \right) / \frac{GM_\star}{r^2} \right|, \end{aligned}$$

These are shown in the figure, although in our approach we do not explicitly solve the momentum equation either.

Note that the gas pressure and the magnetorotational force are almost comparable in the outer region,  $r \gtrsim 10R_\star$ . This shows that it is reasonable to call the wind 'a moderate magneto-rotator'. The figure also illustrates that the wave pressure becomes as effective an acceleration term as these other two components for a magnetorotational wind. This means that the fast wave damping is equally important in the wind dynamics; the waves could further accelerate the wind.

Next, we study effects of rotation rate. In fig. 5, we compare cases of slow rotator ( $S_0 = 0.01$ ) and fast rotator ( $S_0 = 0.5$ ).  $\theta$  is greatly different in both cases as illustrated in a left panel. Accordingly, the waves dissipate more rapidly in the fast rotator (a middle panel), and the heating (and acceleration not shown) occurs in the inner region (a right panel). This indicates that regions heated by the wave dissipation depend on the stellar rotation even when the same waves are input. Generally,  $S_0$  decreases as a star evolves, and then we can speculate that the wave dissipation is controlled by the stellar evolution.

## 4.2. Massive Stars

We have shown that our process possibly works in low mass main sequence stars with moderately fast rotation. In this subsection, we would like to consider cases of massive stars. Traditionally, massive main sequence stars have not been thought to have activities concerning magnetic fields, i.e. coronae and/or flares, because they have surface radiative zone and magnetic fields are expected to be hardly generated by dynamo process. However, as we have stated in §1, coronal activities are speculated in the late B-type stars (Cohen, Cassinelli, & MacFarlane 1997). Furthermore, MacGregor & Cassinelli (2003) showed that the massive stars with the surface radiative zone possibly had surface magnetic fields. Although the coronal like geometry might be rather different from the less massive stars, we consider it interesting and instructive to apply the same basic model to massive stars with extended coronae.

The observed mass-loss rate,  $\dot{M}_{\text{obs}}$ , of these types of stars is known for given  $M_\star$  and  $R_\star$  (de Jager, Nieuwenhuijzen, & van der Hucht 1998). Generally,  $M_E \gtrsim \dot{M}_{\text{obs}}$  in the magnetorotational winds since equatorial mass flux is larger than polar mass flux. Magnetic activities and/or stellar rotation might further enhance intrinsic  $\dot{M}$  as discussed in the previous subsection. To take into account these effects, we consider  $M_E \simeq (1-10)\dot{M}_{\text{obs}}$ . Then, we can construct the wind structure for a certain star after fixing  $B_{r,0}$  and  $S_0$  (§3.1). Here, we would like to introduce a characteristic mass-loss density (Cassinelli et al. 2002) defined as

$$\rho_c \equiv \frac{\dot{M}_E}{R_\star^2 v_\infty}. \quad (23)$$

We have found that  $\rho_c$  is a good indicator for our process; the damping of the fast waves work similarly in

winds with the same  $\rho_c$  but different  $M_*$ ,  $R_*$ , and  $\dot{M}_E$ . This is because the damping is controlled by density in the winds by way of the plasma parameter  $\beta$  which appears in (4) for the damping rate.

We now examine the roles of the fast waves in the wind energetics and dynamics for three stellar parameters,  $\rho_c$ ,  $B_{r,0}$  and  $S_0$ . Since our process does not work dominantly in the slow rotators because the value of  $\theta$  is too small in the winds, we study cases with  $S_0 = 0.15$  (moderate rotator) and 0.5 (fast rotator). We investigate the wave propagation in main sequence stars with  $M_* = 1 - 8M_\odot$ .  $R_*$  for a given  $M_*$  is determined by a relation for the main sequence stars (Kippenhahn & Weigert 1990). Temperature is assumed to be  $T = 2 \times 10^6$  K, independent of  $M_*$ . Several cases of  $\dot{M}_E$  for a fixed  $(M_*, R_*)$  are calculated within the range of  $\dot{M}_E = (1-10)M_{\text{obs}}$ . We consider waves with  $\tau = 1$  s and  $\delta\omega_0 = 0.1$  and investigate how the wave dissipation effectively works in the energetics and dynamics for different  $B_{r,0}$ .

As for the energetics, we examine whether the heating integrated with respect to a certain region exceeds the adiabatic cooling integrated in the same region, namely, we determine the condition of  $B_{r,0}$  which satisfies

$$\int_{R_*}^{r_{\text{out}}} dr \rho r^2 Q_w \geq \int_{R_*}^{r_{\text{out}}} dr \rho a^2 \frac{d}{dr} (r^2 v_r). \quad (24)$$

We adopt  $r_{\text{out}} = 10R_*$  to focus on the heating in the inner wind region. We also carry out the similar procedure for the dynamics. We compare the acceleration due to the wave pressure integrated in the same region with the acceleration by the other two components:

$$\begin{aligned} - \int_{R_*}^{r_{\text{out}}} dr v_r r^2 \frac{dP_w}{dr} &\geq - \int_{R_*}^{r_{\text{out}}} dr v_r r^2 \frac{dp}{dr} \\ &+ \int_{R_*}^{r_{\text{out}}} dr \rho v_r r^2 \frac{d}{dr} \left( \frac{r \Omega B_r B_\phi}{4\pi \rho v_r} \right) \end{aligned} \quad (25)$$

Figure 6 shows the critical values for  $B_{r,0}$  with respect to the energetics (solid; eq. (24)) and dynamics (dashed; eq. (25)) as a function of  $\rho_c$  in the moderate (thick) and fast (thin) rotators. The collisionless damping of the fast modes can dominate the other processes if the field strength exceeds the respective lines. If  $\dot{M}_{\text{obs}}$  is used when deriving  $\rho_c$  instead of  $\dot{M}_E$  in eq. (23),  $\rho_c$  has one-to-one correspondence to  $M_*$  because dependence of  $\dot{M}_{\text{obs}}$  on  $M_*$  is steep (de Jager, Nieuwenhuijzen, & van der Hucht 1998) while those of  $R_*$  and  $v_\infty$  are weaker (Kippenhahn & Weigert

1990). Above the panel, we present a corresponding spectral type of the stars to  $\rho_c$  derived in that manner for reference. Please note that this is based on  $\dot{M}_{\text{obs}}$ . If a star has larger  $\dot{M}_E$  as discussed previously, its  $\rho_c$  becomes larger than the shown spectral type.

The figure shows that the required value for  $B_{r,0}$  is reasonable,  $\sim 10 - 100$  G, for these types of stars (Meheswaran & Cassinelli 1992; Cassinelli et al. 2002). The critical  $B_{r,0}$  is a monotonically increasing function of  $\rho_c$  and a relation,  $B_{r,0}^2 / \rho_c \sim \text{const}$ , holds. Since we assume the same gas temperature, the relation can be understood that the similar plasma  $\beta$  is required even for different stellar mass. As  $\rho_c$  increases, collisionless condition breaks from the inner regions. On dotted lines the plasma is still collisional at  $r = 2R_*$  for the waves with  $\tau = 1$  s. We can conclude that our process can operate effectively in stars with spectral type of late B or later provided that they possess the hot coronae. Interestingly, this is consistent with the result obtained by Cohen, Cassinelli, & MacFarlane (1997) that the X-rays from late B-type stars are inferred due to coronal activities.

In both cases of  $S_0 = 0.15$  and 0.5, the condition for the dynamics demands larger  $B_{r,0}$  than that for the energetics because the former compares the wave acceleration with both thermal and Poynting processes while the latter compare with the thermal processes (i.e. adiabatic cooling) only. In a region between the two conditions, the wind could be heated by the fast waves but is accelerated dominantly by the magnetorotational force rather than by the waves. The wave dissipation is slower in the moderate rotators and a certain fraction of the wave energy remains at  $r_{\text{out}}$ . Therefore, the required  $B_{r,0}$  for the energetics condition is larger than that for the fast rotators to increase the initial wave energy. On the other hand, the dynamics condition shows that the fast rotators demand larger  $B_{r,0}$  to let the wave acceleration exceed the larger magnetorotational acceleration.

## 5. Discussions

So far we have studied outward propagation of the fast waves based on several assumptions : (i) monochromatic wave spectrum (ii) no refraction (iii) fixed magnetorotational winds. First, we discuss these limitations. Then, we compare the collisionless damping and the steepening, and finally we mention another application of our process to pulsar wind nebulae.

### 5.1. Limitation of Model

(i) *Wave Spectrum* : Although we have only considered the monochromatic waves in the model calculation, they are likely to be injected with some spectrum in the real situation, and as we have shown in the previous section, wave frequency controls the wave damping. Namely waves with higher frequencies dissipate in the inner region, and vice versa. If some spectrum (e.g. a power-law in  $\omega$ ) is given for the input waves, the stellar atmosphere is heated more uniformly; inner region is heated by waves with higher frequency and outer region is heated by those with lower one.

(ii) *Wave Refraction* : We have assumed that the fast mode propagates radially without being refracted. In fact, the refraction is not negligible unless the plasma  $\beta$  is sufficiently small. This is because anisotropy of  $v_f$  appears in case that sound speed is not sufficiently small against Alfvén speed (eq. (14)). Generally, a wave is refracted toward a region with a smaller phase speed. As for a fast mode wave, it is refracted in a direction away from the field line (toward larger  $\theta$ ). Thus, this effect causes the wave dissipate earlier since the damping increases with  $\theta$ . As a result, we should expect the heated region to be slightly shifted inward as compared with the assumed radial propagation.

(iii) *Fixed Background* : In this paper, we treat the wave propagation within a given wind structure. We think that this approach is acceptable as a first attempt to estimate the heating and acceleration rates produced by wave dissipation. Needless to say, a self-consistent treatment is required for more sophisticated modeling. The wave dissipation directly affects  $v_r$  (acceleration) and  $T$  (heating), and the other quantities are also modified through these two variables. However, we think that  $v_r$  assumed in the present paper gives reasonable wind structure because it is mainly determined by the stellar parameters,  $M_*$ ,  $R_*$ ,  $S_0$ , and the waves give only a moderate modification to the acceleration profile.

Given this, it is the temperature that must be considered more carefully. Unlike the wind velocity structure, the temperature is not determined by the stellar parameters but rather by the boundary conditions for the wave generation and the subsequent wave heating and radiative cooling and thermal conduction cooling. An important point of our collisionless process is that the damping rate is controlled by temperature through  $\beta$  value (eq. (4)). Once the plasma is heated, i.e.  $\beta$  increase, by the waves, the damping is enhanced. It leads

to further heating until most of the wave energy dissipates, whereas this catastrophic behavior is partially inhibited in reality by thermal conduction which becomes more effective with an increase of temperature. It is important to examine this complicated energetics for more intensive studies.

### 5.2. Collisionless Damping vs. Steepening

We would like to compare the two types of the damping discussed earlier, in light of the magnetorotational wind results. Figure 3 shows that the collisionless process and steepening work in different regimes, namely the former is important for larger  $\theta$  except  $\theta = 90^\circ$  and smaller  $\delta w \lesssim 0.1$  while the latter dominantly works for smaller  $\theta$  and larger  $\delta w > 0.1$ .

In cases of moderate and fast rotator with  $\delta w_0 = 0.1$  (§4), the collisionless damping is expected to operate dominantly in the entire region because  $\delta w$  is small, and thus not suitable for the steepening, in the inner region where  $\theta$  is still small (figs. 4 & 5). However, in slow rotators the shock steepening process is expected to be more important because  $\theta$  does not become large (fig. 5). The shock steepening process would also work effectively even in stars with faster rotation, if the fast waves with large amplitude were injected.

### 5.3. Application to Pulsar Winds

So far we have focused on the collisionless damping of the fast MHD waves in the normal stars. This mechanism can work universally if the fast waves travel in low  $\beta$  plasma with curved magnetic fields. Pulsar wind is one of the candidates. A pulsar magnetosphere is a low  $\beta$  and collisionless plasma, and the MHD approximation is acceptable because the particles can interact through the magnetic fields.

Lyubarsky (2003) considered dissipation of the fast waves propagating radially in pulsar winds by multiple shocks as a result of the steepening in order to investigate dissipation of the electromagnetic energy. Because the toroidal component dominates in the magnetic fields due to the rotation of the pulsars, he studied the fast waves traveling perpendicular to the field lines, i.e.  $\theta = 90^\circ$ . In this case, the collisionless damping is not efficient as shown in §2 so that the steepening is much more effective process in the wave dissipation. However, unless  $\theta$  is strictly  $= 90^\circ$  due to perturbed magnetic fields, etc., the collisionless damping would become important. Although this is beyond the scope

of the present paper, relativistic effects should be taken into account properly to study the collisionless damping in the pulsar winds.

## 6. Summary

For the case of magnetorotationally driven winds, we have considered the heating and acceleration of a stellar plasma caused by the collisionless damping of fast MHD waves. Fast mode waves propagate almost radially even in spiral magnetic fields thanks to the isotropic character of the propagation, provided that the low  $\beta$  condition holds. The plasma is generally collisionless so that the waves undergo collisionless damping. We find that this mechanism is effective when (i) the angle between the wave propagation and the field line is large and (ii) the plasma  $\beta$  is around  $0.01 - 0.1$ . In the magnetorotational winds, the angle increases as the wave travels away from the surface. This angle change eventually leads to a dissipation of the waves, and causes heating and acceleration of the surrounding medium.

We have found that our collisionless damping is important in moderate and fast magnetorotators of solar-mass stars, which implies that it should play a role in the observed coronal activities in young (age  $\lesssim 100$ Myr) solar-type stars. The damping also effectively applies in the energetics and dynamics of atmosphere of main sequence stars of which spectral types are late B or later which have observationally plausible magnetic fields ( $\sim 10 - 100$ G). When compared with the shock dissipation by the steepening, the collisionless damping is expected to be more important in moderate and fast rotators with input wave amplitude,  $\delta w_0 \lesssim 0.1$ . In addition, the process is also argued to be important in general astrophysical low  $\beta$  plasma which has curved magnetic fields, such as pulsar and black hole magnetosphere.

T.K.S. is financially supported by the JSPS Research Fellowship for Young Scientists, grant 4607. A.L. and H.Y. acknowledge NSF grant ATM-0312282, and A.L. and J.P.C., also acknowledge the support of the Center for Magnetic Self-Organization in Laboratory and Astrophysical Plasmas.

### A. Damping by Steepening

In this appendix, we summarize damping of fast shock trains which form by the steepening of the fast MHD waves. First, we derive entropy generation at the fast shock whose geometry is shown in fig. 7. Physical quantities in the upstream region are indicated by subscript '1' and those in the downstream region by '2'. Components parallel with shock normal are denoted by subscript  $\parallel$  and those perpendicular to it by  $\perp$ . Because of the conservation of magnetic flux,  $\nabla \cdot \mathbf{B} = 0$ , parallel components of magnetic field,  $B_{\parallel}$ , is constant. Perpendicular field strength is increased from  $B_{\perp}$  to  $B_{\perp} + \delta B_{\perp}$  at the fast shock. Conservations of mass flux, momentum parallel and perpendicular to shock normal, electric field, and energy are expressed from an observer co-moving with the shock as (e.g. Priest & Forbes 2000)

$$\rho_1 v_{\parallel,1} = \rho_2 v_{\parallel,2}, \quad (\text{A1})$$

$$p_1 + \rho_1 v_{\parallel,1}^2 = p_2 + \rho_2 v_{\parallel,2}^2 + \frac{2B_{\perp}\delta B_{\perp} + \delta B_{\perp}^2}{8\pi}, \quad (\text{A2})$$

$$\rho_1 v_{\parallel,1} v_{\perp,1} = \rho_2 v_{\parallel,2} v_{\perp,2} - \frac{B_{\parallel}\delta B_{\perp}}{4\pi}, \quad (\text{A3})$$

$$v_{\parallel,1} B_{\perp} - v_{\perp,1} B_{\parallel} = v_{\parallel,2} (B_{\perp} + \delta B_{\perp}) - v_{\perp,2} B_{\parallel} (= 0) \quad (\text{A4})$$

and

$$\begin{aligned} p_1 v_{\parallel,1} + \rho_1 e_1 v_{\parallel,1} + \frac{B_{\perp}^2}{4\pi} v_{\parallel,1} - \frac{B_{\parallel} B_{\perp}}{4\pi} v_{\perp,1} + \frac{1}{2} \rho_1 (v_{\parallel,1}^2 + v_{\perp,1}^2) v_{\parallel,1} \\ = p_2 v_{\parallel,2} + \rho_2 e_2 v_{\parallel,2} + \frac{(B_{\perp} + \delta B_{\perp})^2}{4\pi} v_{\parallel,2} - \frac{B_{\parallel} (B_{\perp} + \delta B_{\perp})}{4\pi} v_{\perp,2} + \frac{1}{2} \rho_2 (v_{\parallel,2}^2 + v_{\perp,2}^2) v_{\parallel,2}. \end{aligned} \quad (\text{A5})$$

Transformation of eqs.(A1)–(A5) gives a relation between  $\delta B_{\perp}$  and compression ratio,

$$\sigma \equiv \frac{\rho_2}{\rho_1}, \quad (\text{A6})$$

as

$$-\frac{\gamma p_1}{\rho_1} \frac{\sigma - 1}{\sigma} - \frac{\delta B_{\perp}^2}{8\pi\sigma\rho_1} + \{\gamma + 1 - \sigma(\gamma - 1)\} \frac{\delta B_{\perp}}{8\pi\sigma\rho_1} \frac{\{(\sigma - 1)B^2 - B_{\perp}\delta B_{\perp}\}}{\{\delta B_{\perp} - (\sigma - 1)B_{\perp}\}} = 0 \quad (\text{A7})$$

Pressure jump is also derived from eq. (A2) :

$$\Delta p \equiv p_2 - p_1 = \frac{2(\sigma - 1)B^2\delta B_{\perp} + (\sigma - 3)B_{\perp}\delta B_{\perp}^2 - \delta B_{\perp}^3}{8\pi\{\delta B_{\perp} - (\sigma - 1)B_{\perp}\}}, \quad (\text{A8})$$

where  $B^2 = B_{\parallel}^2 + B_{\perp}^2$ . Entropy generation is written as

$$\frac{\Delta s}{R} = \frac{1}{\gamma - 1} \{\ln(1 + \frac{\Delta p}{p}) - \gamma \ln(\sigma)\}, \quad (\text{A9})$$

where  $R$  is a gas constant. Then,  $\Delta s$  is derived from a given amplitude,  $\delta B_{\perp}$ , by using eqs.(A7) and (A8). The steepening of the wave fronts form the fast shock train. The wave dissipates by these multiple shocks. Heating rate,  $Q_s$ (erg cm $^{-3}$ s $^{-1}$ ), of the fast shock train with angular frequency,  $\omega$ , is given by

$$Q_s = \frac{\Delta s}{R} \rho_1 R T \frac{\omega}{2\pi} = \frac{\Delta s}{R} p_1 \frac{\omega}{2\pi}. \quad (\text{A10})$$

Damping rate is derived from  $Q_s$  and energy density of the wave,  $\frac{\delta B_{\perp}^2}{8\pi}$ , as

$$\gamma_s = \frac{Q_s}{\delta B_{\perp}^2/8\pi} \quad (\text{A11})$$

## REFERENCES

Barnes, S. A. 2003, *ApJ*, 586, 464

Belcher, J. W. 1971, *ApJ*, 168, 509

Belcher, J. & MacGregor, K. B. 1976, *ApJ*, 210, 498

Boyd, T. J. M. & Sanderson, J. J. 2003, *The Physics of Plasmas*, Cambridge

Cassinelli, J. P., Brown, J. C., Maheswaran, M., Miller, N. A., & Telfer, D. C. 2002, *ApJ*, 578, 951

Cassinelli, J. P. & Olson, G. L. *ApJ*, 1979, 229, 304

Cassinelli, J. P. & Swank, J. H. *ApJ*, 1983, 271, 681

Charbonneau, P., & MacGregor, K. B. 2001, *ApJ*, 559, 1094

Cho, J. & Lazarian, A. *MNRAS*, 2003, 345, 325

Cohen, D. H., Cassinelli, J. P. & MacFarlane, J. J. 1997, *ApJ*, 487, 867

Donati, J.-F., Wade, G.A., Babel, J., Henrichs, H.F., de Jong, J.A., & Harries, T.J. 2001, *MNRAS* 326, 1265

Ginzburg, V. L. 1961, *Propagation of Electromagnetic Waves in Plasma*, New York: Gordon & Breach

Hartmann, L. & MacGregor, K. B. 1980, *ApJ*, 242, 260

Henrichs, H.F. 2001, in *Magnetic Fields across the Hertzsprung-Russell Diagram* ASP Conf Ser. Vol 248, 393

Hollweg, J. V. 1982, *ApJ*, 254, 806

Jacques, S. A. 1977, *ApJ*, 215, 942

de Jager, C., Nieuwenhuijzen, H., & van der Hucht, K. A. 1998, *A&AS*, 72, 259

Kippenhahn, R. & Weigert, A. 1990, "Stellar Structure and Evolution", *Springer-Verlag*

Lamers, H. J. G. L. M. & Cassinelli, J. P. 1999, 'Introduction to Stellar Wind', Cambridge

Lamers, H. J. G. L. M. & Morton, D. C. *ApJS*, 1976, 32, 715

Leamon, R. J., Mattheaeus, W. H., Smith, C. W., & Wong, H. K. 1998, *ApJ*, 507, L181

Lucy, L. B. 1982, *ApJ*, 255, 286

Lyubarsky, Y. E. 2003, *MNRAS*, 339, 765

MacGregor, K. B. & Cassinelli, J. P. 2003, *ApJ*, 586, 480

Michel, F. C. 1967, *ApJ*, 158, 727

Maheswaran, M. & Cassinelli, J. P. 1992, *ApJ*, 386, 695

Owocki, S. P. 1994, *Ap&SS*, 221, 3

Parker, E. N. 1963, 'interplanetary Dynamical Processes', John Wiley and Sons, New York

Parker, E. N. 1966, 145, 811

Parker, E. N. 1975, 198, 205

Priest, E. & Forbes, T. 2000, *Magnetic Reconnection*, Cambridge

Seward, F. D., Forman, W. R., Giacconi, T., Griffiths, R. E., Harnden, F. R., Jr., Jones, C., & Pye, J. P. 1979, *ApJ*, 234, L55

Sturrock, P. A. 1999, *ApJ*, 521, 451

Suzuki, T. K. 2004, *MNRAS*, 349, 1227

Waldron, W. L. & Cassinelli, J. P. 2000, *ApJ*, 548, 145

Weber, E. J. & Davis, L. 1967, *ApJ*, 148, 217

Wood, B. E., Müller, H.-R., Zank, G. P., & Linsky, J. L. 2002, *ApJ*, 574, 412

Yan, H. & Lazarian, A. 2004, *ApJ*, 614, 757

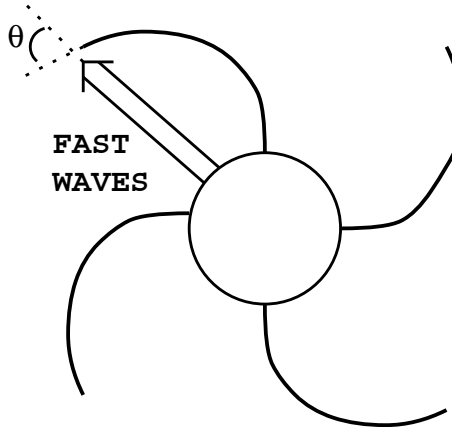


Fig. 1.— Schematic picture of fast MHD waves in magnetorotational wind.

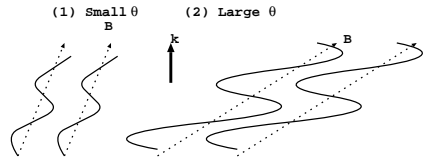


Fig. 2.— Propagation of fast MHD waves for different  $\theta$ . In low  $\beta$  plasma, fluctuation of the fast mode is almost perpendicular to propagation direction denoted by  $k$  vector. Figure illustrates that magnetic mirror is effectively formed for larger  $\theta$ .

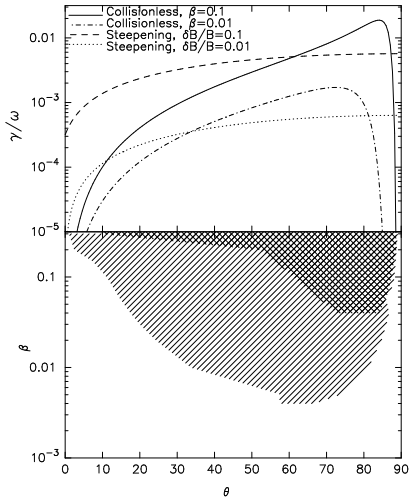


Fig. 3.— *upper*: Comparison of damping rate of the collisionless process with the steepening as a function of  $\theta$ . *lower* : Regions in  $\theta - \beta$  where the collisionless process dominates the steepening for  $dB/B = 0.1$  (cross hatched) and  $dB/B = 0.01$  (single hatched).

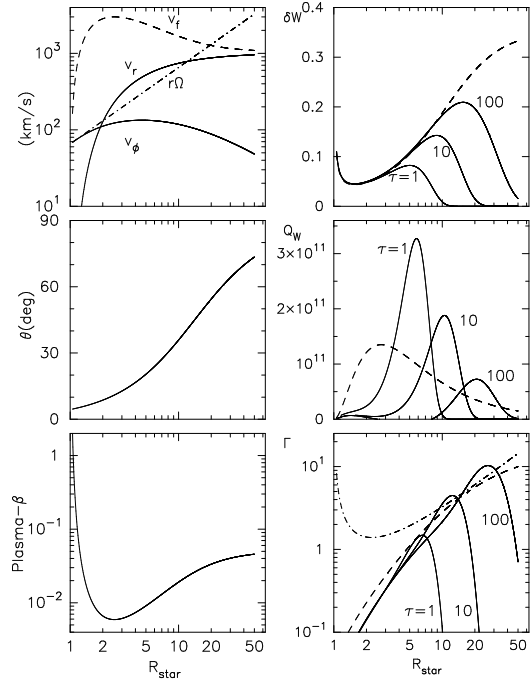


Fig. 4.— Wave dissipation in a solar-type star with  $S_0 = 0.15$ . All the physical quantities are as a function of stellar radius. *Upper left* : velocity structure. *Middle left* :  $\theta$ . *Lower left* : plasma  $\beta$  value. *Upper right* : Normalized amplitude of the fast waves. Solid lines are results with dissipation for three cases of wave period,  $\tau$ . Dashed line is a result without dissipation. *Middle right* : Comparison of heating,  $Q_w$ (erg/g s), for the three  $\tau$ 's (solid) with adiabatic cooling in eq. (21) (dashed). *Lower right* : Comparison of  $\Gamma$ . Solid lines are wave acceleration,  $\Gamma_w$ , dashed line is magnetorotational acceleration,  $\Gamma_b$ , and dot-dashed line is acceleration by gas pressure,  $\Gamma_g$ .

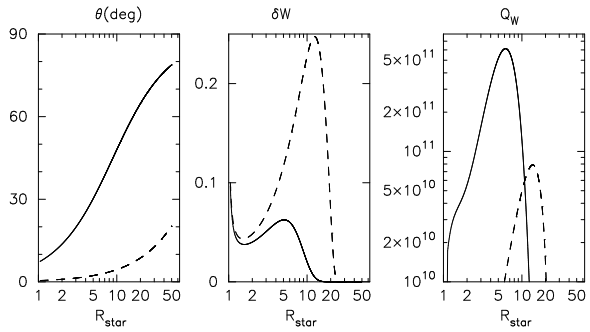


Fig. 5.— Comparison of fast ( $S_0 = 0.5$ ; solid) and slow ( $S_0 = 0.01$ ; dashed) rotators. We plot  $\theta$ ,  $\delta w$ , and  $Q_w$ (erg/g s) from left to right.

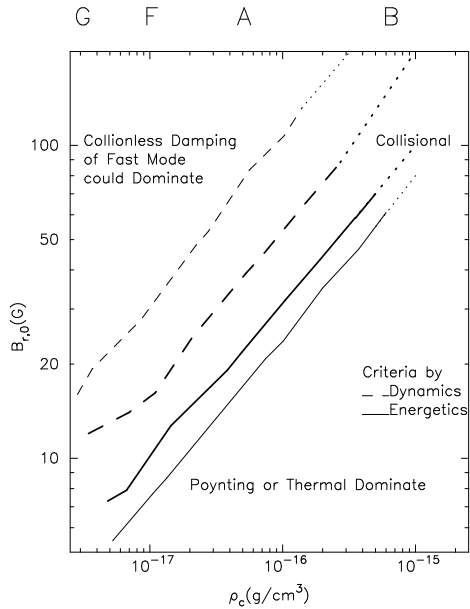


Fig. 6.— Critical magnetic field for collisionless damping of the fast waves as a function of characteristic density,  $\rho_c$  for spin parameter  $S_0 = 0.15$  (thick) &  $0.5$  (thin). We here consider the waves with  $\tau = 1$ (s) and  $\delta w_0 = 0.1$ . Solid lines indicate criteria based on the energetics and dashed lines are those of the dynamics. Upper characters on the top denote corresponding main sequence stars (see text). In upper left region of each line the wave dissipation gives larger contributions to the heating or acceleration than the other processes. In upper right region which is indicated as 'Collisional', the plasma is still collisional even at  $r = 2R_*$  due to high density so that our process does not work effectively.

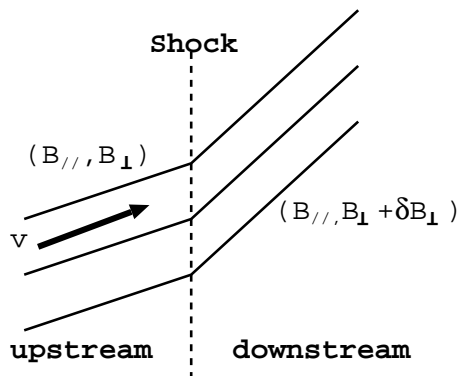


Fig. 7.— Geometry of fast shock.